JOURNAL OF AIRCRAFT
Vol. 33, No. 1, January–February 1996

Cratering Phenomena on Aircraft Anti-Icing Films

J. La Due,* M. R. Muller,† and M. Swangler‡
Rutgers University, Piscataway, New Jersey 08903

This article reports on a study of cratering effects in thin anti-icing films designed to protect aircraft surfaces from snow and ice accumulation while the aircraft is on the ground awaiting takeoff. These fluids primarily consist of a glycol used as a freezing point depressant, water, and to a small extent thickening and wetting agents. Craters formed in these films represent local areas where the film thickness is dramatically reduced and can lead to premature failure of the film. This phenomenon was found to be driven by surface tension gradients at the film surface that cause surface movement and drag the underlying fluid. These surface tension gradients are formed because the surfactants being used in the anti-icing fluids are more effective in water-rich solutions than in glycol-rich solutions. Experimental results are given that illustrate this behavior of the surfactant and numerical work is presented to show that the magnitude of surface tension differences obtained is adequate to drive the phenomenon.

Nomenclature

C	= concentration of surfactant
G_0	= Gibbs' free energy
G^*	= ratio of gravity-to-surface tension gradient forces
g	= gravitational constant
H_0	= initial film thickness
P	= pressure
R_0	= radius of surface tension gradient area
r	= radial coordinate
S	= spreading parameter, $\sigma_0 - \sigma_m$
t	= time
$u(r, z)$	= radial velocity
$w(r, z)$	= axial velocity
z	= axial coordinate
ε	= ratio of axial-to-radial length scale
μ	= Newtonian viscosity
ρ	= density
σ	= surface tension
σ_m	= minimum in surface tension within the diluted region, $0 < r < R_0$
σ_0	= surface tension of anti-icing fluid

I. Introduction

GROUND icing on aircraft awaiting takeoff during freezing precipitation is a major safety concern. Current practice at airports is to combat ground icing in two ways. Deicing fluids are designed to be applied hot to the aircraft structure to provide chemical and thermal melting of any accumulated ice on the aircraft structure. Historically, these fluids were a pure mixture of water and glycol and offered little protection against additional precipitation. To increase the time over which an aircraft had protection against freezing precipitation, these type I fluids have been engineered to create type II fluids, which are intended for anti-icing applications. These fluids are thickened to increase their effectiveness, but are shear thinning to allow them to shear off as the aircraft reaches rotation speeds to produce a clean wing on takeoff.

The time between the application of the anti-icing fluid and its failure to inhibit the formation of ice is designated as the holdover time, or HOT. Degradation of an anti-icing fluid refers to its reduction in ability to melt incoming precipitation, thereby resulting in film failure. It was long believed, in the absence of any comprehensive field evaluation of the fluids, that the degradation of the anti-icing films was caused simply by increased dilution of the film, which led to film thinning due to runoff and eventual failure.

Recently, field studies[1] (funded by the Federal Aviation Administration) were undertaken to determine holdover times for various anti-icing fluids under differing ground icing conditions. The testing indicated that the type of simple analysis previously held on the film degradation did not apply. Figure 1 represents the variation in failure time with precipitation rate for anti-icing fluids accumulated during the 1990–91 icing season. The general trend of the data is, as expected, that the holdover time decreases as the precipitation rate increases. However, the scatter of data, especially at the low precipitation rate end, is very large. One explanation[2] for the variability is that several different modes of failure can occur. In some cases the momentum of the incoming precipitation is so low that it does not mix into the anti-icing fluid. In other cases the momentum of the incident precipitation is high and subsequent mixing with the fluids occurs. These complexities can contribute to the scatter seen. However, the momentum of the incoming precipitation is not the only variable affecting the different types of degradation seen. In certain cases, there are anomalies associated with the precipitation–fluid system itself.

One such anomaly stems from observations made during field testing of type II anti-icing fluids during the winter of 1990. The field study was intended to determine holdover time and contributed to the results of Fig. 1. It was observed in some cases that an unusual form of degradation occurred whereby craters were produced in the film during a precipitation event characterized by ice pellets. The formation of these craters led to localized areas in the film where the thickness was reduced dramatically. These localized areas then represented regions where film failure occurred prematurely and led to a reduction in the capability of the anti-icing film to protect the aircraft surfaces from snow and ice.

The focus of this article is the study of this cratering mode of degradation. In order to achieve the highest performance of the type II thickened anti-icing fluids, the cause of this mode of degradation must be isolated. It is then that the fluids can be re-engineered to inhibit this mode from occurring. To fully

Presented as Paper 95-0893 at the AIAA 33rd Aerospace Sciences Meeting and Exhibit, Reno, NV, Jan. 9–12, 1995; received Feb. 11, 1995; revision received Aug. 1, 1995; accepted for publication Aug. 10, 1995.

*Research Associate, Department of Mechanical and Aerospace Engineering. Student Member AIAA.

†Professor of Mechanical Engineering, Department of Mechanical and Aerospace Engineering.

‡Research Assistant, Department of Mechanical and Aerospace Engineering.

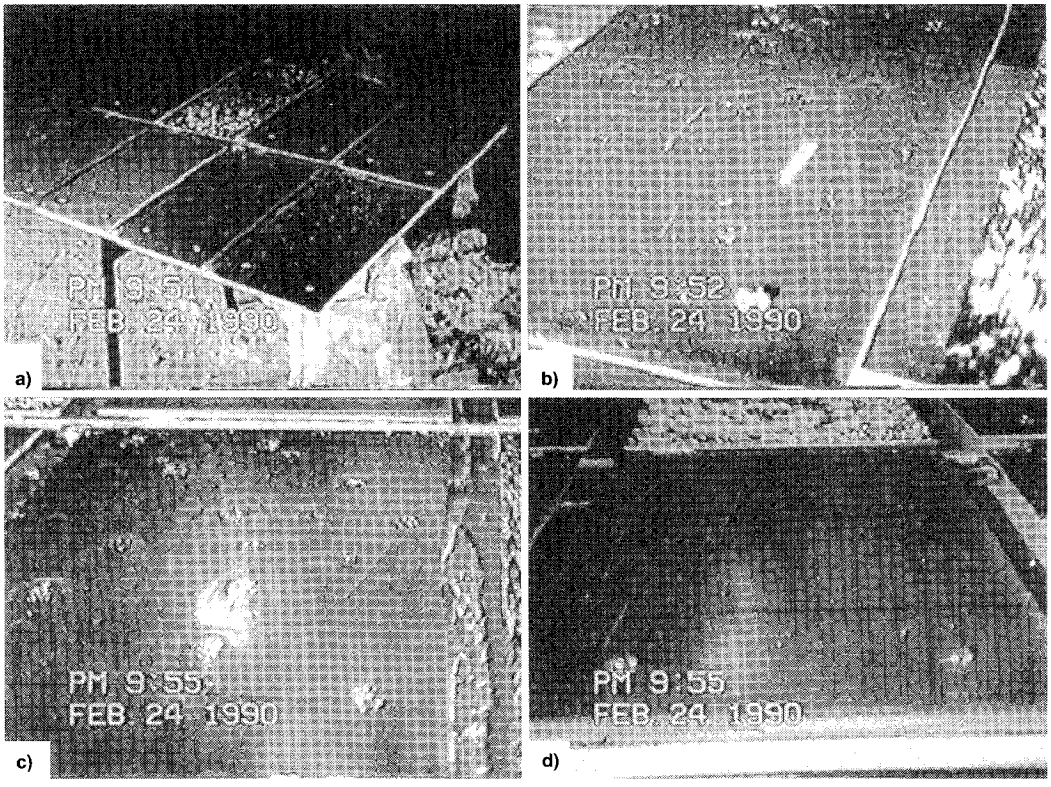

Plate 1 Field testing, Hamilton, New York.

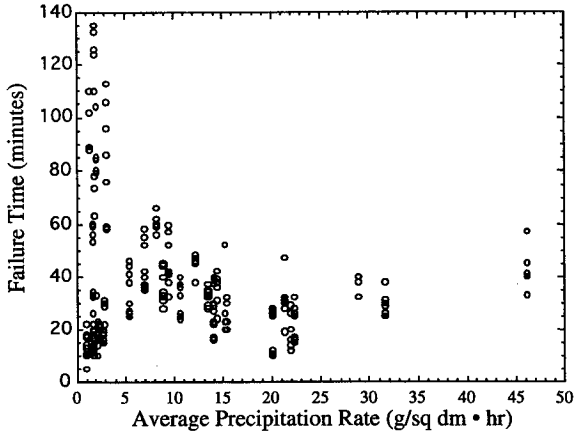

Fig. 1 Variation in failure time with precipitation rate accumulated from field testing.[1]

understand the effect, some background into the composition of the anti-icing fluids is warranted.

II. Composition of Anti-Icing Fluids

The base of the composition of the anti-icing fluids consists of the freezing point depressant (FPD). The FPD in most anti-icing fluids is either ethylene or propylene glycol.[3,4] The purpose of the freezing point depressant is to cause chemical melting of the incoming precipitation. This allows its removal from the flight surfaces as the aircraft reaches takeoff speeds. Freezing point depressants often comprise 50–70% of the total composition by volume of the anti-icing fluid. Water comprises 30–50% of most anti-icing fluids. Because of the high miscibility between water and the glycols, consistent solutions can be obtained. As previously noted, a distinguishing feature of type II anti-icing fluids as compared to the type I de-icing fluids is the thickening agent. The purpose of the thickening agent is to increase the viscosity of the anti-icing fluid to dramatically slow runoff, or drainage. This allows the fluid to achieve higher thicknesses while on the aircraft, and thus, theoretically increase the holdover time. The thickening agents used in the fluids are proprietary in nature. However, their basic function is primarily the same in all anti-icing fluids; to thicken the fluid, yet allow it to shear off as rotation speed is approached. To this end, long chain polymers are often used, which when present in small concentrations (1–5%), can dramatically thicken the fluid and achieve non-Newtonian shear thinning behavior. B. F. Goodrich manufactures a wide variety of Carbopol™ thickening agents that hydrate and swell when introduced into a water environment, and hence, have high thickening characteristics.[5]

An important constituent of anti-icing fluids and critical to this research is the wetting agent, or surfactant. The purpose of the wetting agent is to decrease both the interfacial tension between the fluid and the substrate and the surface tension of the fluid to allow for spontaneous spreading wetting of the fluid over the aircraft surfaces.[6] This allows the anti-icing fluid to coat the aircraft surfaces properly. It will be shown later that improper choices for surfactants can be the basis for the cause of the crater formation process studied.

III. Field Testing

Field studies exhibiting cratering effects are illustrated in Plate 1. These photographs were taken during an icing event in Hamilton, New York in 1990.[2] Color views of these plates can be found in an earlier work.[7] The precipitation at the time could be characterized by a mixture of snow and ice pellets. In Plate 1a the experimental apparatus can be seen that consisted of eight plates mounted on a 10-deg angle of inclination onto which several different anti-icing fluids are poured and then exposed to freezing precipitation. One of the plates, used as a control, had no anti-icing fluid protection and can be seen to be rapidly covered in snow. The test plates shown in Plates 1b and 1c project an unusual feature. At certain points where ice pellets had fallen on the test plate, the anti-icing fluid ap-

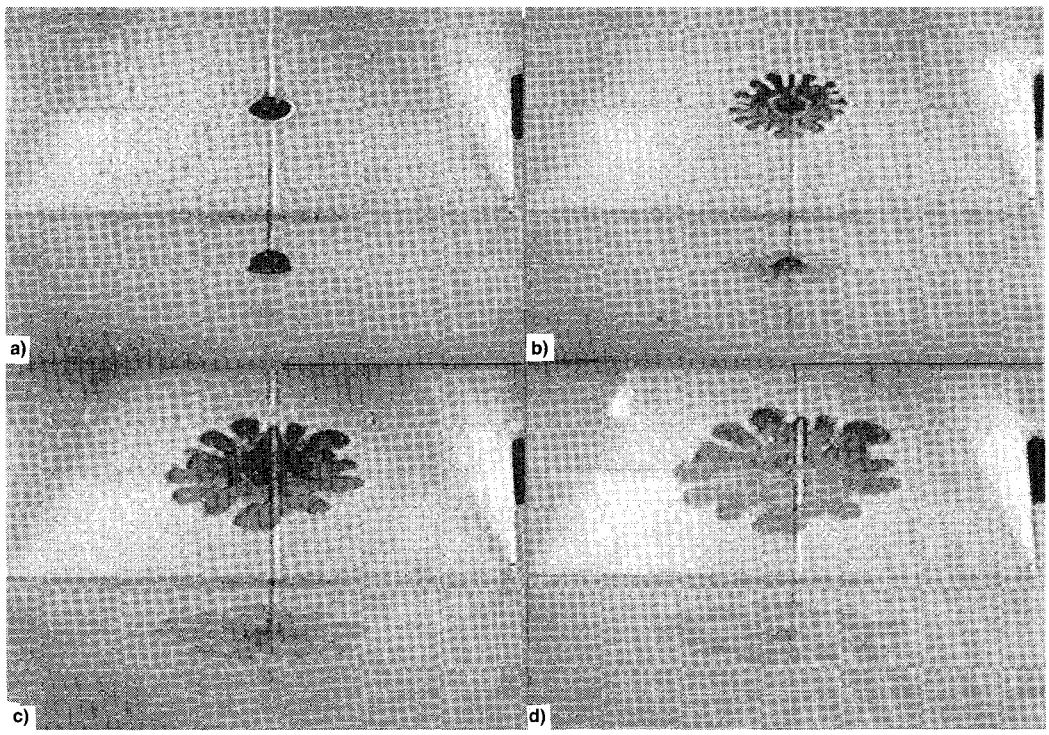

Plate 2 Laboratory simulation of crater formation.

pears to have been pushed away from the ice pellet, forming a crater leaving a very thin coating of anti-icing fluid below. This area is shown to be rapidly filling with snow at a rate similar to that of the control plate. Clearly, the formation of craters led to premature failure of the plates and it is therefore important to understand their generation. However, this effect is not inclusive to all anti-icing fluids as Plate 1d illustrates. Here, no cratering effects can be seen for this anti-icing fluid.

IV. Laboratory Experiments

As a result of the field study an attempt was made to reproduce the observed cratering phenomenon in the laboratory. A plate identical to those used in the field studies was placed in the freezer. To allow for modeling of the system at a later time, no tilt of the plate was used. A commonly used type II anti-icing fluid was poured over the plate and a mechanical blade coater was used to achieve a uniform thickness. Round ice pellets were obtained by immersing drops of water in a sub-freezing oil bath. The oil was then stripped from the pellet by partially melting it in a water bath, resulting in a round, clean ice pellet. To create a red appearance for better flow observation, a rhodamine dye was added to the drops, resulting in a dyed ice pellet. Typically, several of these pellets were placed on the fluid-coated plate and allowed to melt chemically. If the film thickness was sufficiently thin, craters very similar to those seen in the field studies were observed. Plate 2 shows a series of four photographs showing the sequence of events. Here, a mirror is placed atop the fluid so that the simultaneous viewing from the top and side can be seen. In Plate 2a an ice pellet is placed on the film/substrate system and melts under the action of chemical melting with the FPD. In Plate 2b partial melting of the ice pellet is seen. The water released from the pellet spreads rapidly over the fluid to form a beautiful pattern indicative of a fingering instability.[8,9] Laboratory experiments have indicated that the water-rich area spreads over the top of the film without significant penetration into the film due to its buoyant nature. This has also been verified by concentration measurements.[10] In Plate 2c the advancement of the outer edge of the water-rich area slows dramatically. In Plate 2d a roughly circular crater that forms in the diluted region can be seen.

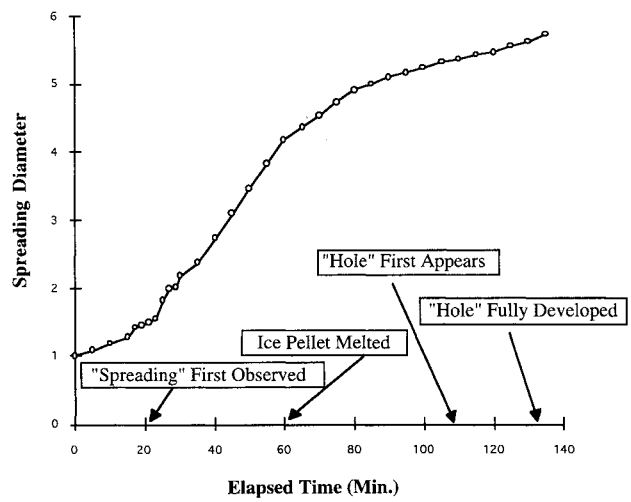

Fig. 2 Graphical representation of laboratory experiment.

Here the ice pellet has melted, the water-rich fluid has spread over the anti-icing fluid, and a crater is formed.

The steps to this process are illustrated graphically in Fig. 2 where a large ice pellet and extremely cold temperatures are used to slow the process dramatically.[2] As can be seen in this graph, the spreading is initially rapid, but then slows at which time the hole is seen to first appear.

A schematic of the surface profile of the film during the process can be seen in Fig. 3. In Fig. 3a the ice pellet is seen atop the anti-icing film and melts under the action of the FPD. In Fig. 3b partial melting of the ice pellet is seen along with an initial start of the cratering process. The piling up of the fluid at the crater edge can be seen here. A fully developed crater is seen in Fig. 3c. The size of the crater reaches a quasi-equilibrium value where little variation in size occurs over long periods of time. In time scales of several hours, which is far greater than holdover times encountered for ground aircraft, craters that initially form do eventually close, leading to a flat film surface that can be seen in Fig. 3d. The final stage of the

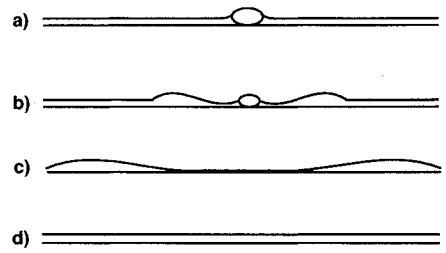

Fig. 3 Schematic of experimental crater formation process.

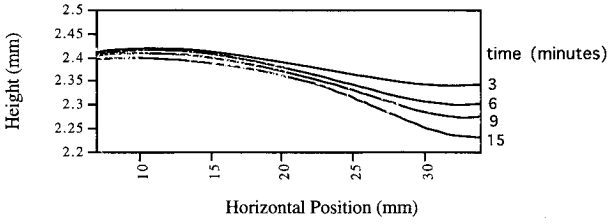

Fig. 4 Experimentally measured surface profile using noncontact refractometry.

cratering formation process is thus not directly applicable to the ground icing problem.

The experimental surface profile during the cratering process has also been carefully monitored over time. Figure 4 is a diagram indicating the surface profile of the anti-icing film during the cratering process as measured by a noncontact refractometry method. In this test, a water droplet serves to induce the crater formation rather than an ice pellet. Here, rapid thinning in the center of the region is seen over time along with the characteristic piling of the fluid at the crater edge. Of special note in this figure is the time scale involved in the process that indicates the rapid growth that can occur even for the cold temperatures involved in icing events.

V. Driving Mechanism

When considering the mechanisms that could cause a crater to form in thin anti-icing fluid, it is important to consider what effects could drive the phenomenon and which will oppose the process. Gravity, in the form of hydrostatic pressure gradients, would obviously have an overall leveling effect on the film surface, and thus, would oppose crater formation.

Capillary (surface tension) forces with origins in the curvature of the free surface always act to reduce the area of the film surface and may act to open or close holes formed, depending on whether the process increases or decreases the surface area. The concept of a critical radius, below which a hole will close and above which a hole may open, has been examined in detail by Taylor and Michael[11] and later by Schwartz and Moriarty,[12] who used a more dynamic model. Application of their models to this problem indicates a critical radius of ice pellet many times the diameter of the ice pellets used, and hence, capillary forces alone are not large enough to generate the crater.

Therefore, neither gravity nor surface tension forces are possible mechanisms, leaving surface tension gradient, or Marangoni,[13,14] forces the most likely driving mechanism. These surface tension gradients can cause surface movement that drags the underlying fluid due to viscous effects and cause craters to form. It is important to note that surface tension flows are from regions of low surface tension towards regions of high surface tension. Thus, in the cratering problem, in order for surface tension gradients to drive the effect the diluted region must exhibit a lower surface tension than the pure anti-icing fluid. This is apparently counterintuitive since pure water that can result from the melting of an ice pellet has a surface tension of 73 dyne/cm, which is approximately 40 dyne/cm larger than the surface tension of pure anti-icing fluid (32 dyne/cm). In addition, binary mixtures of water and glycol, the two main components of anti-icing fluids, never have a surface tension lower than the anti-icing fluid because of the lack of surfactant. Therefore, the key to the creation of a low surface tension area must lie in the action of the surfactant in the diluted region. In order to fully understand this, some background will be given on surfactant performance.

VI. Surfactant Performance

In determining the performance of surfactants in reducing surface tension in a given solvent it is necessary to consider the concentration of surfactant present in the solution. For extremely dilute surfactant systems, the surface tension reduction scales with the concentration of surfactant molecules present at the interface. This concentration is a well-known function of the free energy change associated with the surfactant molecule moving from the bulk to the interface and can be expressed as[15]

$$C_{\text{interface}}/C_{\text{bulk}} = \exp[(-\Delta G_0)/RT] \tag{1}$$

This characteristic associated with the free energy change upon adsorption is referred to as the surfactant efficiency.

As the amount of surfactant added to the bulk of the fluid increases, a limit is reached where additional molecules are unable to reach the surface. Any increase in concentration beyond this point typically results in the formation of micelles within the bulk of the fluid. This bulk concentration in which this occurs is referred to as the critical micelle concentration, or CMC.[16] The particular CMC of a surfactant/solvent system depends on both the surfactant efficiency and the maximum packing that the surfactant can achieve at the interface. Together, these are referred to as the surfactant effectiveness. Figure 5 is a schematic representation showing typical surface tension changes with increasing bulk concentration. As surfactant is added to the bulk, increased adsorption results in a decreasing of surface tension with surfactants having higher efficiencies in the solvent used exhibiting larger surface concentrations for a given bulk concentration. A characteristic break in the curve exists at the CMC. The interface is considered to be saturated with surfactant below, but near the CMC, the closest packed arrangement of surfactant molecules at the interface achieved with the amount of surfactant molecules entering and leaving the interface in a given time interval equal.[15] The surface tension remains essentially constant above the CMC since only the monomeric form of the surfactant at

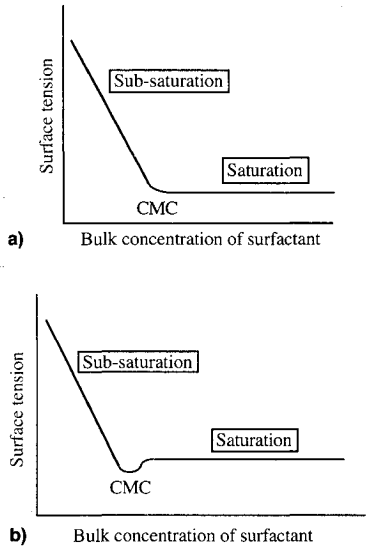

Fig. 5 Behavior of surfactant with bulk concentration: a) no impurities and b) with trace impurities.

the interface contributes to the reduction in surface tension. Occasionally, a minimum in surface tension can be seen as in Fig. 5b, which is due to the presence of trace amounts of impurities often existing in real solutions.[17] These impurities can be adsorbed at the surface and reduce surface tension slightly until the CMC is reached. It is then that the micelles can solubilize impurities removing them from the surface resulting in a slight increase in surface tension after the CMC is reached.

It is important to note that many surfactants are significantly more effective in lowering surface tension when dissolved in water as compared to glycols. This is due to the strong polar nature of water as compared to the relatively weak polar nature of glycols. Surfactants have a dual structure consisting of a lyophobic group (the tail), which has very little attraction for the solvent and a lyophilic group (the head), which has a strong attraction for the solvent. For surfactants used in polar solvents, the lyophobic grouping, or the tail, usually consists of a nonpolar molecular chain. When a surfactant molecule is dissolved in a highly polar solvent the presence of the nonpolar tail dramatically increases the free energy of the system. This free energy can be minimized by the surfactant molecule moving to the interface and lowering the surface tension resulting in the free energy change described earlier. Often, with weakly polar solvents such as glycols, the surfactant molecules when dissolved in the system do not increase the free energy significantly, and thus, have little tendency to accumulate at the interface and lower surface tension. It is this effect that can account for the reduced effectiveness of many surfactants when used in glycols rather than in water. This effect is illustrated in Fig. 6, which shows surface tension measurements made by the DuNuoy ring method of a nonionic surfactant that exhibits this variable performance in solutions with a varying percentage of ethylene glycol and water as solvent. Note that as the concentration of ethylene glycol in the solvent increases, the efficiency of the surfactant decreases as more surfactant must be added to the bulk to get a given amount of change in surface tension. This is reflected in the slope of the $\partial\sigma/\partial \log C$ curve. A change in the CMC can also be seen with a change in the amount of glycol present.[18] A minimum in surface tension can be seen in these charts, which is apparently due to the presence of trace amounts of impurities described earlier.

This effectiveness reduction due to the presence of ethylene glycol in the solvent is illustrated when a surfactant-rich post-CMC solution is constructed with the solvent comprised of a mixture of ethylene glycol and water in varying percentage. This is illustrated in Fig. 7 where it can be seen that with ample surfactant present, the total effectiveness of the surfactant in lowering surface tension, is reduced when the ethylene glycol/water ratio is increased.

When considering the performance of a surfactant in an anti-icing fluid it is important to note that the anti-icing fluids are post-CMC,[19] and thus, always attain the maximum surface concentration when the interface is allowed to come to equilibrium. It is also important to note that the surfactants used in these fluids are proprietary, and hence, cannot be independently evaluated in concentrations below CMC as in the preceding section. However, it is clear that the family of surfactants used in the anti-icing fluids that exhibit cratering behavior has a greater effectiveness in water than in ethylene glycol. Quite simply, a solution of water and surfactant would have a lower surface tension than a solution of ethylene glycol and surfactant.

Information on the effectiveness of the surfactants used in anti-icing fluids as a function of solvent composition can be achieved when anti-icing fluids, which are composed primarily of water and glycol as previously mentioned, are diluted with water. Figure 8 illustrates the surface tension measurements made by the DuNuoy ring method for an anti-icing fluid diluted in water (fully mixed), which exhibits cratering effects. As can be seen from the plot, with low concentrations of the

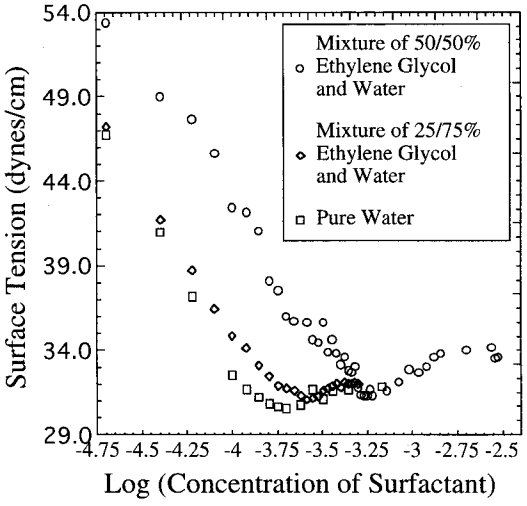

Fig. 6 Variation in surface tension with bulk concentration for TRITON-X® (Union Carbide Corp.) surfactant.

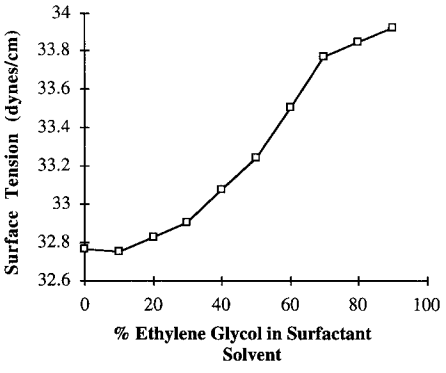

Fig. 7 Variation in surface tension with variation of amount of ethylene glycol in solvent.

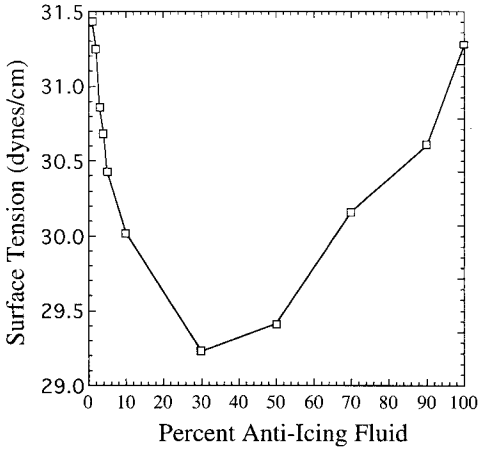

Fig. 8 Variation of surface tension when anti-icing fluid is diluted with water.

anti-icing fluid in water, the effect of the added surfactant present in the anti-icing fluid increases adsorption at the interface, resulting in a decrease in surface tension as the concentration of the anti-icing fluid increases.

However, the process does not continue as the concentration of anti-icing fluid is increased. At a certain point during the process the interface becomes saturated with surfactant and the effect of the added ethylene glycol in the anti-icing fluid dominates and reduces the effectiveness of the surfactant by the effects described earlier, thus resulting in an increase in surface

tension. Hence, water diluted regions can exhibit lower surface tensions resulting in surface tension gradient induced flows with crater formation. Ice pellets, representing a continual supply of water during the phase change process, can create these concentration gradients leading to the Marangoni-induced motion. Localized dilution by ice pellets during the degradation process has also been observed in an independent study done by Hansman.[20]

VII. Surfactant Transport

Since diluted regions rich in surfactant achieve lower surface tension than the surrounding fluid, the question of how the surfactant migrates into the diluted region arises. Experimental results indicate that the surfactant transport mechanism is rapid as a water drop placed on the anti-icing film begins to spread nearly instantaneously, which can only occur, neglecting the effect of gravitational spreading, if $S > 0$. This requires that the edge of the diluted region achieves an abrupt drastic reduction in surface tension. In addition, the fingering instability that develops during the spreading process is consistent with previous work done[8,9] in both the direction and pattern of the fingers, indicating the spreading of a low surface tension region. Thus, experimental evidence would suggest a rapid transport mechanism.

Advection, or the movement of the surface in response to a surface tension gradient, is one such fast transport mechanism. Flow visualization experiments indicate that if a drop of water is placed on an anti-icing film, the surface movement is initially inward before an outward spreading of the drop is seen. This is to be expected as surface tension flows are from low to high and the surface tension of pure water is approximately 40 dyne/cm larger than the anti-icing fluid used. This inward flow, however, is very transient as the rapid inward movement carries with it surfactant from the surrounding anti-icing fluid, thus lowering the surface tension in the diluted region. Hence, rapid advection is a mechanism that can equalize the surface tension between the diluted region and the anti-icing fluid.

For the surface tension of the diluted region to get lower than the surrounding fluid, some other mechanism must be responsible for surfactant transport. It has been experimentally ascertained that diffusion of surfactant into the diluted region is a very slow process and could not account for the additional transport needed in the time scales of the crater formation process. However, there is significant mixing between the anti-icing fluid and the diluted region during the spreading process. This mixing can transport small amounts of surfactant to the interface, which is most likely responsible for saturating the interface of the diluted region with surfactant resulting in the lower surface tension there. Thus, the transport of surfactant consists of two primary mechanisms: 1) rapid surface advection, which transports the surfactant from surface movement inward and 2) some mixing that occurs as the diluted region spreads.

It is important to note that the time scales involved with these two mechanisms are small and it is generally convenient to consider the interface of the diluted region to be saturated with surfactant when the radius of the diluted region reaches its quasiequilibrium value.

VIII. Preliminary Numerical Work

Analysis of Fig. 8 reveals that the surface tension differences encountered in diluted regions are subtle. The early numerical modeling of the crater formation process has been devoted to verifying that a surface tension variation in the anti-icing fluid upon dilution of the small magnitude seen could be responsible for the craters seen experimentally. To achieve this, a model for the crater formation process had to be developed. This model is presented here.

Because the problem at hand will deal with axisymmetric holes, a two-dimensional coordinate system will be adopted. A simple schematic of the two-dimensional system is seen in Fig. 9. Here the ice pellet is replaced by a diluted region of high water concentration of R_0, which has spread over the infinite anti-icing fluid film of H_0. The fingers that form during the spreading process are neglected in this representation of the problem.

Although laboratory experiments have indicated that R_0 never reaches a constant value, a quasiequilibrium value is reached where the spreading slows dramatically, and hence, the radius of the region is taken to be constant. The ratio of capillary driving forces to surface tension gradient forces is taken to be small, and hence, capillary forces are neglected. The diluted region will be assumed to be saturated with surfactant with the surface tension lower than the surrounding anti-icing fluid due to the high water concentration present. The velocity in the radial direction will be designated as u and in the axial direction as w. The gravitational body force is acting in the negative z direction. The anti-icing fluids are treated as Newtonian, which is a valid approximation for the very low shear rates encountered in the cratering process.[21]

The scaled variables for this model are[22,23]

$$z^* = z/H_0, \quad r^* = r/R_0, \quad \sigma^* = (\sigma - \sigma_m)/S, \quad u^* = u/u_1$$
$$w^* = w/\varepsilon u_1, \quad P^* = (P - P_0)/(S/H_0), \quad t^* = t/(R_0/u_1) \tag{2}$$

where $S = \sigma_0 - \sigma_m$ is the spreading parameter that is the maximum difference in surface tension between the diluted region and the surrounding anti-icing film and $\varepsilon = H_0/R_0 \ll 1$ and $u_1 = \varepsilon S/\mu$, which is the velocity scale found by scaling the balance of tangential stress at the interface caused by surface tension gradients.[22] For such a model, the governing equation for the evolution of the film height $H(r, t)$ subject to gravitational leveling and driven by surface tension gradients within R_0 can be shown to be[22,23]

$$\frac{\partial H^*}{\partial t^*} = \frac{1}{r^*}\frac{\partial^*}{\partial r^*}\left[r^*\left(G^*\frac{H^{*3}}{3}\frac{\partial H^*}{\partial r^*} - \frac{H^{*2}}{2}\frac{\partial \sigma^*}{\partial r^*}\right)\right] \tag{3}$$

where $G^* = \rho H_0^2 g/S$ represents the ratio of gravity to surface tension gradient (Marangoni) forces.[22] Here, the thin film approximation is in place, namely, that $\varepsilon = H_0/R_0 \ll 1$, and as such, terms of $\mathcal{O}(\varepsilon^2)$ are neglected.

To ascertain if the magnitude of the surface tension differences obtained are adequate to drive the craters formed, the numerical work involves the solution of the nonlinear film evolution Eq. (3), subject to the appropriate boundary conditions with an imposed surface tension distribution in the diluted region. Although unknown, this distribution must satisfy the condition of zero gradient at the edge of the diluted region as indicated by the radius of the region reaching a quasiequilibrium value, which can only occur if S approaches zero. A distribution that satisfies this condition consists of a variation of surface tension from $0 < r^* < 1$ that has the magnitude of the maximum variation determined from the static surface tension measurements and varies smoothly in the following manner:

$$\sigma^*(r^*) = \tanh(ar^*) \tag{4}$$

where the parameter a controls the steepness of the gradient.

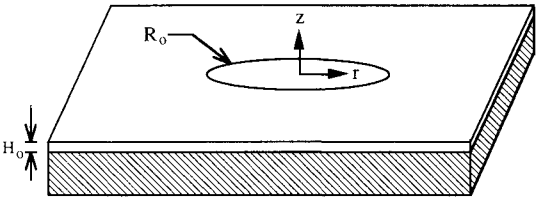

Fig. 9 Representation of crater formation model.

Table 1 Time conversion

Nondimensional time	Corresponding dimensional time, s
0.05	31.25
0.1	62.5
0.2	125.0
0.4	250.0
0.8	500.0
1.0	625.0
1.2	750.0

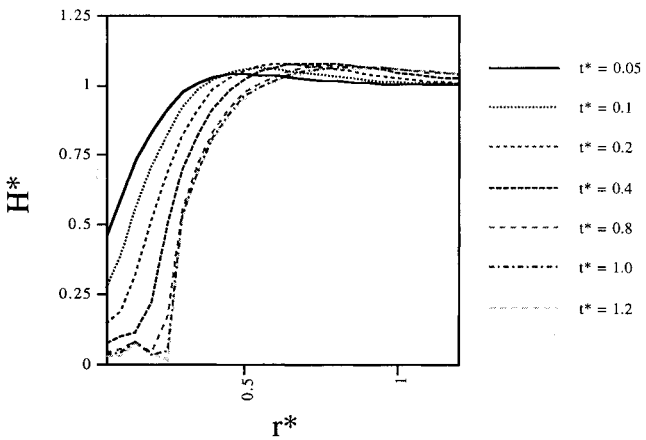

Fig. 10 Numerically calculated surface profiles with imposed surface tension gradient (a = 3).

Note that this type of analysis does not include surface advection or diffusion that can cause variations in the surface tension distribution as the film evolves, and hence, is only valid for early times.

The film evolution equation with the imposed gradient can be solved via the method of lines.[24,25] The results for the numerical output for the case when $a = 3$ can be seen in Fig. 10. As the chart illustrates, the value of nondimensional time varies from 0.05 to 1.2 as the film free surface evolves under the imposed surface tension gradient. H^* represents the nondimensional film height where the initial nondimensional film height at time zero is unity. R^* represents the nondimensional radial distance when the imposed gradient occurs in $0 < r^* < 1$. Values for the nondimensional parameters used in the case were arrived at by using characteristics of the icing system under study. An average shear rate of 0.041 s^{-1} was calculated assuming a linear velocity profile throughout the thin film to determine an average viscosity for this Newtonian approximation to the non-Newtonian anti-icing film. The following are the conditions used for the study:

Temperature, 0°C
Shear rate, 0.041 s^{-1}
Associated viscosity, 6 Pa-s
Fluid density, 1070 kg/m^3
R_0, 1.0 cm
H_0, 0.4 mm

Using the previous values, the value for the real times corresponding to the nondimensional times is shown in Table 1. Thus, using parameters characteristic of the system, a significant crater can form very shortly after the region establishes a low surface tension.

IX. Summary

This study has shown the role of the surfactant in the dynamics of cratering in thin anti-icing fluids. Ice pellets can create localized areas where the surface concentration of water is increased. The high effectiveness of the surfactant in these areas creates localized regions of lower surface tension, which drives Marangoni convection at the surface, which drags the underlying fluid resulting in cratering. Diffusion of these diluted regions into the surrounding fluid can relieve these surface tension gradients leading to the closing of craters, but on time scales much larger than aircraft holdover times. Experimental surface tension measurements have verified this behavior of the surfactant with solvent concentration and numerical work has indicated that the magnitude of the variations can create large disturbances in the film. This study has shown that the cratering observed is apparent in most anti-icing fluids, but is not inclusive. It is clear then that the thickened type II anti-icing fluids that exhibit this cratering effect should be redesigned to prevent this mode of degradation from occurring. In this way their effective protection of the aircraft surfaces is maximized. This may include a change of surfactant or perhaps a favorable mixture of surfactants, but in either case the result should be a more constant surface tension when the glycol/water ratio is varied in the fluid.

Acknowledgments

The authors would like to acknowledge the support of the FAA Technical Center's Aircraft Icing Program and the FAA-Rutgers Fellowship Program and to B. F. Goodrich, Union Carbide, ARCO, Texaco, Dow, and Kilfrost Limited for their donation of chemicals.

References

[1]Muller, M. R., and Polomski, P. P., "Field Studies of Hold-Over-Times for Type II Anti-Icing Fluids: Results and Insights," AIAA Paper 93-0749, Jan. 1993.

[2]Muller, M. R., and La Due, J. C., "An Experimental Study of Cratering Effects in Thin Liquid Anti-Icing Films," 12th U.S. National Congress of Applied Mechanics, Seattle, WA, June 1994.

[3]"Use and Handling Overview of KILFROST ABC-3 Propylene Glycol Aircraft Anti-Icing Fluid," ARCO Chemical Publication and Material Safety Data Sheet, ARCO Chemical, Inc., Newtown Square, PA, 1993.

[4]"UCAR Aircraft Anti-Icing Fluid for Safe Winter Operations," Material Safety Data Sheet and Qualification Test Rept., Union Carbide, Anjou, PQ, Canada, 1993.

[5]*Carbopol Resins Handbook*, B. F. Goodrich Technical Publication, Cleveland, OH, 1991.

[6]Garrett, H. E., *Surface Active Chemicals*, Pergamon, New York, 1972, pp. 36–39.

[7]La Due, J., Muller, M. R., and Swangler, M., "A Study of Dynamic Cratering Effects in Thin Anti-Icing Films," AIAA Paper 95-0893, Jan. 1995.

[8]Troian, S. L., Wu, X. L., and Safran, S. A., "Fingering Instability in Thin Wetting Films," *Physical Review Letters*, Vol. 65, 1989, pp. 1406–1408.

[9]Troian, S. M., Herbolzheimer, E., and Safran, S. A., "Model for the Fingering Instability of Spreading Surfactant Drops," *Physical Review Letters*, Vol. 65, 1990, pp. 333–336.

[10]Muller, M. R., Polomski, P. P., and La Due, J. C., "Anti-Icing Failure Detection Instrumentation Using Real-Time Optical Measurement of Anti-Icing Fluid Properties," AIAA Paper 93-0748, Jan. 1993.

[11]Taylor, G. I., and Michael, D. H., "On Making Holes in a Sheet of Fluid," *Journal of Fluid Mechanics*, Vol. 58, Pt. 4, 1973, pp. 625–639.

[12]Schwartz, L. W., and Moriarty, J. A., "Dynamic Considerations in the Closing and Opening of Holes in Thin Liquid Films," *Journal of Colloid and Interface Science*, Vol. 161, No. 2, 1993, pp. 335–338.

[13]*Chemistry and Physics of Interfaces II*, American Chemical Society Publications, Washington, DC, 1971, pp. 56, 57.

[14]Sternling, C. V., and Scriven, L. E., "Interfacial Turbulence: Hydrodynamic Instability and the Marangoni Effect," *Journal of the Association of Industrial and Chemical Engineering*, Vol. 5, No. 4, 1959, pp. 514–523.

[15]Rosen, M. J., *Surfactants and Interfacial Phenomena*, Wiley, New

York, 1978, pp. 27, 60.

[16]Lucassen-Reynders, E. H., *Anionic Surfactants: Physical Chemistry of Surfactant Action*, Marcel Dekker, New York, 1981, pp. 57, 58.

[17]Davies, J. T., and Rideal, E. K., *Interfacial Phenomena*, Academic, New York, 1961, pp. 200, 201.

[18]Mitsunobu, O., Kato, K., and Kimura, J., "Micelle Formation in Pure Ethylene Glycol," *Journal of the American Chemical Society*, Vol. 91, No. 23, 1969, pp. 6511, 6512.

[19]Boluk, Y., private communication, Union Carbide Corp., Jan. 1992.

[20]Anagnostakis, I., Khayms, V., and Hansman, R. J., "Microphysical Observations of Precipitation Impact and Melting of Non-Newtonian De-Icing Fluids," AIAA Paper 95-0657, Jan. 1995.

[21]Perron, E., Louchez, P. R., and Laforte, J. L., "Study of the Shearing of Ground De-Icing and Anti-Icing Fluids," AIAA Paper 95-0658, Jan. 1995.

[22]Graver, D. P., and Grotberg, J. B., "The Dynamics of a Localized Surfactant on a Thin Film," *Journal of Fluid Mechanics*, Vol. 193, 1990, pp. 127–148.

[23]Halpern, D., and Grotberg, J. B., "Dynamic and Transport of Localized Soluble Surfactant on a Thin Film," *Journal of Fluid Mechanics*, Vol. 237, 1992, pp. 1–11.

[24]Hicks, J. S., and Wei, J., "Numerical Solutions of Parabolic Partial Differential Equations with Two-Point Boundary Conditions by Use of the Method of Lines," *Journal of the Association of Computing Machinery*, Vol. 14, No. 3, 1967, pp. 549–562.

[25]Holt, M., *Numerical Methods in Fluid Dynamics*, Springer–Verlag, New York, 1984, pp. 233–249.